

Structural, UV-VIS-NIR luminescence and decay associated spectral profiles of Sm³⁺ doped calcium phosphate glass

Sooraj H. Nandyala^{1,2*}, Graham Hungerford³, J. L. Rao⁴, Isabel B. Leonor^{1,2}, Ricardo Pires^{1,2}, Rui L. Reis^{1,2}

¹ICVS/3B's, PT Government Associated Laboratory, Braga/Guimarães, Portugal

²3B's Research Group – Biomaterials, Biodegradables and Biomimetics, University of Minho, Headquarters of the European Institute of Excellence on Tissue Engineering and Regenerative Medicine, Avepark, Barco, 4805015 Guimarães, Portugal

³HORIBA Jobin Yvon IBH Ltd., 133 Finnieston Street, Glasgow G3 8HB, United Kingdom

⁴Department of Physics, Sri Venkateswara University, Tirupati 517502, Andhra Pradesh, India

*Corresponding author. Tel: (+351) 933420872; E-mail: nandyala.sooraj@gmail.com

Received: 25 October 2015, Revised: 05 February 2016 and Accepted: 25 May 2016

ABSTRACT

The present paper reports a calcium phosphate host glass doped with 2 mol% of samarium oxide (2Sm). The glass has been characterized by FTIR, SEM, EDS analysis, and X-ray mapping. Exciting in the visible, using 405 nm and 423 nm, we observed intense, sharp green, yellow, orange emission peaks ($^4G_{5/2} \rightarrow ^6H_{5/2, 7/2, 9/2}$) at 560nm, 596 nm and 643 nm respectively. A weak red emission was also observed at 704 nm. Two NIR peaks at 1134nm ($^4G_{5/2} \rightarrow ^6F_{11/2}$) and 1310 nm ($^4G_{5/2} \rightarrow ^6F_{9/2}$) are monitored by using an excitation at 1060 nm. Furthermore, by making use of time-resolved emission spectroscopy (TRES) measurements, enabled the decay associated spectra to be obtained and the kinetic parameters for the different emission bands to be determined for comparison with steady state emission spectra. Copyright © 2016 VBRI Press.

Keywords: Sm³⁺ glass; time resolved emission spectra; decay associated spectra; calcium phosphate glass.

Introduction

Phosphate glasses can be advantageous as they exhibit low melting points, glass transition and softening temperatures. In spite of solubility drawbacks, their low processing temperatures have promoted their use in different applications [1] and preference for calcium phosphate based materials has increased for hard tissue engineering and bone graft applications. Because they are major inorganic constituents of hard tissues in the body they can also act as act as motivators. They are generally used in a dense, granular or porous form, as well as composites for the coating of metal prostheses and implants. Improvement in the osteoblast response in the inorganic part of bone can be achieved in several ways, including the use of osteoconductive glass-reinforced hydroxyapatite (GR-HA) composites. These create an ideal environment for bone cells adhesion and proliferation, enabling better bone regeneration [2, 3]. Lanthanides, also known as Rare-Earths [4, 5], are a group of elements from lanthanum to lutetium (Z=57 to 71), plus scandium (Z=21) and Yttrium (Z=39) with a great similarity to calcium. Lanthanides can be divided into three groups: the light lanthanides (lanthanum to samarium), the transition group lanthanides (europium, gadolinium, terbium) and the heavy lanthanides (dysprosium to lutetium) [6, 7]. Lanthanide substituted calcium phosphate helps in improving the biological activity compared to the unsubstituted product and

overcomes the problem to target radionuclide to the bone [8-10]. Webster *et al.* have reported the response of osteoblasts to hydroxyapatite doped with divalent and trivalent cations [11]. Previously the authors have reported the use of Sm³⁺ doped calcium phosphate host glass reinforced hydroxyapatite composites for bone tissue applications [12]. These composites show a good degree of biocompatibility, further enhancing the cell adhesion and proliferation behaviour. Sm³⁺(4f⁵) ions are often luminescent and the orange-red luminescence transition originates from the $^4G_{5/2}$ level to the ground state $^6H_{5/2}$ and to other j- manifolds of the 6 H term. Furthermore, in terms of luminescence trivalent lanthanide ions provide an alternative to the use of organic dyes in view of their emission properties i.e. long luminescence lifetime, narrow full width at half maximum (FWHM) of their emission peaks, and large stokes shift [13]. Sm-doped crystals and glasses are well-known as being the basis for efficient luminescent materials enabling new colour emitting phosphors, with high room temperature quantum yields, as well as high thermal and chemical stability, to be developed [14].

To be able to identify either enhanced or new optical devices research is ongoing selecting appropriate new hosts doped with different lanthanides. The addition of Nd³⁺ ions coupled with the spectroscopic properties of lithium borate glasses is suggestive that this could provide a suitable

system for 1.06 μm infrared laser applications [15]. Addition of Sm^{3+} ions increases the density of glasses due to creation of BO_4^- units [16]. Previous work by the authors has addressed the structural and photoluminescence studies of different host glasses [17-21]. Time-resolved emission spectroscopy (TRES) enables the emission spectra to be determined at specified times during the decay [20]. This provides a technique, which is suitable to study the structure via the kind of active ion present and its local environment, i.e. its local site and distribution within the host material. [20]. Therefore, the present paper reports on the structural, UV-VIS- NIR emission and time-resolved emission spectral profiles of Sm^{3+} doped calcium phosphate glass.

Experimental

Fabrication of the Sm^{3+} doped calcium phosphate host glass

Sm_2O_3 doped calcium phosphate glass has been prepared by the quenching technique. Briefly, the glass was obtained by melting the mixture of analytical grade CaF_2 , Na_2CO_3 , CaO , P_2O_5 , and Sm_2O_3 raw chemicals (Sigma Aldrich, 99.99% purity), in crucible for about an hour in an electrical furnace at a temperature of 1000-1100 $^\circ\text{C}$, with the following chemical composition; 2Sm: 10 CaF_2 -10 Na_2CO_3 -15 CaO -63 P_2O_5 -2 Sm_2O_3 . The resultant glass was circular in design with 2-3 cm in diameter, with a thickness of 0.33-0.38 cm and with good transparency. The glass was then annealed at 200 $^\circ\text{C}$ for an hour to remove thermal strains.

Characterization techniques for Sm^{3+} doped calcium phosphate host glass

Glass density ($\rho = 2.6\text{g}/\text{cm}^3$) was measured using water as an immersion liquid by Archimedes' principle on Mettler Toledo balance. X-ray diffraction (XRD) was performed on powder samples for both glasses and composites by using Siemens D 5000 diffractometer with $\text{Cu-K}\alpha$ radiation ($\lambda = 1.5418\text{\AA}$). The scans were made in the range of 25-40 $^\circ$ (2 θ) with a step size of 0.02 $^\circ$ and a count time of 2 sec/step. Fourier transform infrared (FTIR) spectra was recorded using KBr pellets in the range of 400-4000 cm^{-1} at a resolution of 4 cm^{-1} on a Jasco FT/IR - 460 PLUS spectrophotometer. The spectrum was recorded by using the KBr pellets containing approximately 95 % of KBr and 5 % of glass sample in 250 mg of a pellet. Before recording the spectra, the samples were dried in a Buchi Glass Oven- B-585, at 120 $^\circ\text{C}$, for 1 hour. Raman spectra was record in the back scattering geometry, at room temperature with 514.53 nm polarised line of an Ar^+ laser excitation, with an incident power of about 150 mW. The spectral slit width was $\sim 1.5\text{ cm}^{-1}$ and the spatial resolution on the sample will be about 1 μm . SEM imaging and colour coded X-ray mapping were performed in a FEI Quanta 400 FEG ESEM/EDAX Genesis X4M, a high resolution environmental Scanning Electron Microscope with X-ray microanalysis and backscattered electron diffraction pattern analysis. Both, SEM images and mappings were obtained in a high vacuum mode and with an acceleration of 500 kV. In order to avoid superficial charge accumulation, the sample was covered with a carbon film. X-ray maps

were acquired in regions of 500 x 400 μm for a period of 15 minutes.

Time-resolved measurements for Sm^{3+} calcium phosphate host glass

Measurements in the visible wavelength region were performed on a HORIBA Scientific Delta Flex equipped with Delta Diode laser excitation sources (emitting at 405 nm & 423 nm), Spectra LED sources (emitting at 246nm & 259 nm) and a PPD-850 detector. Those in the NIR were obtained using a HORIBA Scientific FluoroCube, again with Delta Diode excitation (1060nm), and using a H10330-75 detection module close coupled to the timing electronics using a CFD-2G amplifier / discriminator. The Delta Diode excitation sources were operated in "burst mode" with the 100 MHz excitation pulse chain automatically gated using the Data Station software. Time-resolved emission spectra (TRES) were made by recording the time-resolved decay at equal wavelength steps for a fixed time period. This produced an intensity - wavelength - time, i.e 3-D, dataset. Both simple decay and global analysis of the TRES data was performed using DAS6 software. Decays were fitted as a sum of exponential components of the form;

$$I(t) = \sum_i^n \alpha_i \exp(-t/\tau_i) \quad (1)$$

With the "amount" of each luminescent component represented by the normalised pre-exponential factor, i.e;

$$\alpha_i = \frac{\alpha_i}{\sum_{i=1}^n \alpha_i} \quad (2)$$

Single decay data were also treated using a lifetime distribution model (NED module in DAS6) as described earlier [20, 21]. Goodness of fit was assessed by evaluation of the reduced chi-squared value and weighted residuals. The outcomes of the global analysis of the TRES data were then treated to produce decay associated spectra by plotting (using Origin software) the pre-exponential components (see eq. 2), weighed by their lifetime, against wavelength.

Results and discussion

Structural profiles of Sm^{3+} doped calcium phosphate host glass

The amorphous nature of the Sm^{3+} doped calcium phosphate glass was observed by X-ray diffractometer (XRD) (data not shown). The presence of Sm ions was confirmed by EDX data in the calcium phosphate host glass as shown in **Fig. 1(A)**. The surface morphology of the calcium phosphate glass at magnification of 10000 X was given in the inserted SEM image, **Fig. 1(B)**. This shows that the Sm^{3+} glass sample appears homogeneous at the observed magnification. **Fig. 1(C)** shows the x-ray mapping of EDX layer (global area) image and the inserted image represent the samarium mapping, **Fig. 1(D)**.

The chemical structure of the Sm^{3+} doped calcium phosphate glass was analyzed by both FTIR and Raman studies. As seen from the **Fig. 2A**, the band at about

1290 cm^{-1} is assigned to asymmetric stretching modes, ν_{as} (PO_2) of the two non-bridging oxygen atoms bonded to a phosphorus atom in Q2 phosphate tetrahedron [22]. The absorption bands $\nu_{\text{as}}(\text{P-O-P})$ and $\nu_{\text{s}}(\text{P-O-P})$ occurring about 900 cm^{-1} and 750 cm^{-1} are assigned, respectively, to the asymmetric and symmetric stretching modes of the bridging oxygen atoms bonded to a phosphorus atom.

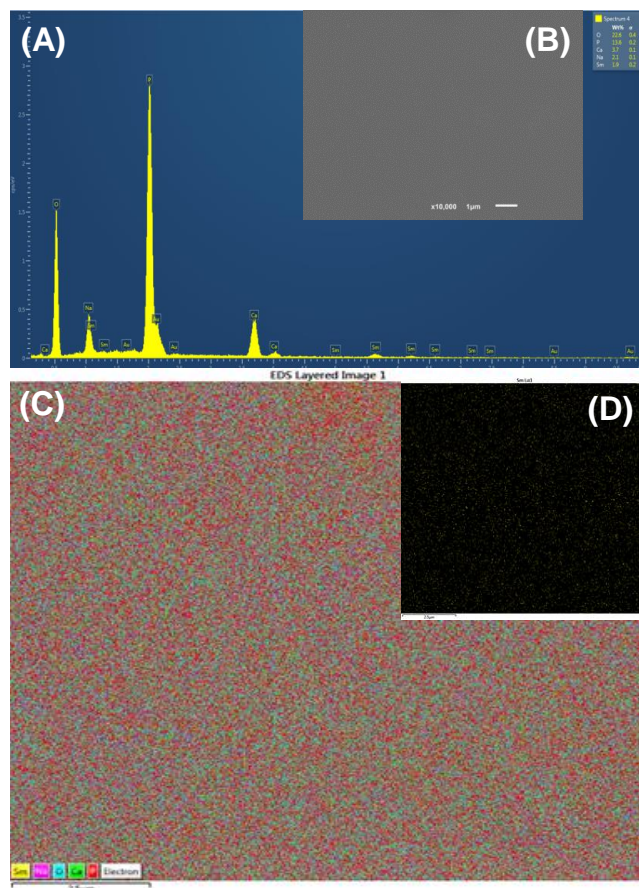


Fig. 1. (A) EDX spectrum of Sm^{3+} doped calcium phosphate glass; (B) The inserted SEM image shows with the magnification at (10000x); (C) X-ray mapping images of global area; (D) Samarium mapping.

The bands at around 444 – 462 cm^{-1} can be ascribed to deformation modes of PO_4^{3-} groups. The broad IR feature at 750 cm^{-1} is assigned to symmetric stretching modes of P–O–P linkages. The absorption band at around 3500 cm^{-1} mainly relates to the free OH groups present in the glass matrix. In order to confirm these results, Raman analysis was also performed. **Fig. 2B** shows the Raman spectra for the prepared Sm^{3+} glass. It is possible to observe the presence of three main regions; in the range 600 – 900 cm^{-1} , 1100 – 1300 cm^{-1} and 1500 – 1800 cm^{-1} . These regions can be assigned, respectively, to the vibrations of P–O–P bonds, symmetric vibration of the middle chain (PO_2) $^-$ and vibrations of the P–O double bond [23]. In pure P_2O_5 glasses, there are two main bands at 1390 cm^{-1} and 640 cm^{-1} . The first band is assigned to the P=O vibrations and it can shift around 70–90 cm^{-1} with the addition of alkali oxides to the Sm sample. This outcome is in good agreement with the bands observed in the spectra shown. This is the result of the delocalization of bonds in Q³ tetrahedra, from the P=O terminal oxygen bond to the bridging P–O–P oxygen bonds [24]. The band at around

1170–1180 cm^{-1} is also characteristic of the alkali oxides added to P_2O_5 glasses, and it increases with the oxide content [23–25].

UV-VIS–NIR luminescence and decay profiles of Sm^{3+} doped calcium phosphate host glass

In order to verify the dependence of luminescence spectra based on the excitation wavelengths of the 2 Sm glass, it was excited at four different excitation wavelengths (246 nm, 259 nm, 405 nm and 423 nm).

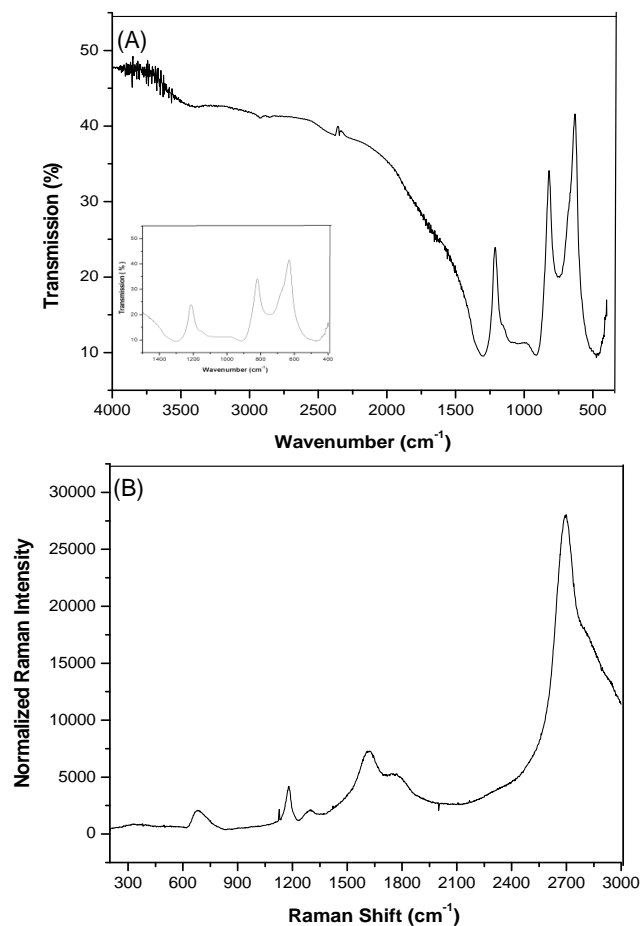


Fig. 2. (A) FTIR spectrum and inserted image shows the 400–1400 nm; (B) Raman spectrum of Sm^{3+} doped calcium phosphate host glass.

The emission spectra of the Sm^{3+} - doped calcium phosphate host glass have shown (**Fig. 3**) the following four visible emission transitions, $^4\text{G}_{5/2} \rightarrow ^6\text{H}_{5/2}$ (560 nm, Green); $^6\text{H}_{7/2}$ (596 nm, Yellow); $^6\text{H}_{9/2}$ (643 nm; Orange) and $^6\text{H}_{11/2}$ (704 nm, Red). Among these four bands, the $^4\text{G}_{5/2} \rightarrow ^6\text{H}_{7/2}$ one is more dominant (Yellow emission). A similar trend was also observed in other fluorophosphates host glasses reported in the literature [26]. A violet emission was also observed from UV excitation (246 nm, 259 nm). Such a comparative study reveals that 405 nm (visible) excitation wavelength could be identified as more suitable for generating strong yellow-orange phosphorescent emission from this 2Sm glass. Similarly, the samarium glass was excited at 1060 nm in the NIR region and exhibited two broad NIR peaks at 1134 nm ($^4\text{G}_{5/2} \rightarrow ^6\text{F}_{11/2}$) and 1310 nm ($^4\text{G}_{5/2} \rightarrow ^6\text{F}_{9/2}$), as shown in the

Fig. 3B. The corresponding NIR peaks and respective lifetime decay curves are shown as inserted images. The transitions ${}^4G_{5/2} \rightarrow {}^6F_{11/2,9/2}$ have a lifetime of 1.1 and 2.1 microseconds respectively and enables these NIR peaks to have potential application in the area of optical communication systems, optical switching and bio-imaging.

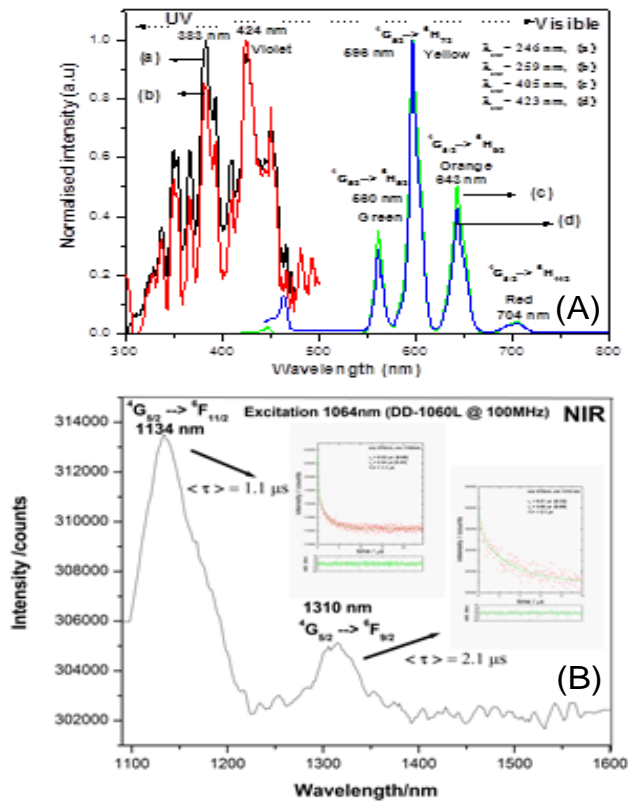


Fig. 3. (A) UV-visible emission spectra; (B) NIR emission spectrum; inserted images show lifetimes of the corresponding peaks.

The **Fig. 4A** shows the decay curves (sum decays) of the 2Sm glass. In a simple exponential way (i), the luminescence intensity $I(t)$ is well modelled by the sum of two exponential decay components i.e., $I(t) = \alpha_1 \exp(-t/\tau_1) + \alpha_2 \exp(-t/\tau_2)$ where τ_1 and τ_2 are the short and long lifetimes with corresponding pre-exponentials α_1 and α_2 , respectively. The decay and recovered data are given in the **Fig. 4A**. Another form of analysis is to consider a distribution of lifetimes and this has previously been reported for doped glass materials [20] and can represent a range of microenvironments within the host matrix. The decay data were fitted using the non-extensive decay distribution module in the DAS6 data analysis software. The model employed is based on Tsallis non-extensive statistics [27] and has been used to interpret time-resolved fluorescence decays by Włodarczyk and others [28]. A more recent report using this type of model is given by Rolinski and Birch [29]. This gives a fit based on:

$$I(t) = A + \sum B_k \left[1 - (1 - q) \frac{t}{\tau_k} \right]^{\frac{1}{1-qk}} \quad (3)$$

where, $k=1$ to 5, τ_k is the mean value of the lifetime distribution and q is a parameter of heterogeneity defined by:

$$q = 1 + \frac{2}{N} = 1 + \frac{\langle (\gamma - \langle \gamma \rangle)^2 \rangle}{\langle \gamma \rangle^2} \quad (4)$$

which relates to the width of the distribution and the number of decay channels (N), based on a γ function, the results of this form of analysis are shown graphically with the area under the distribution given normalised to the pre-exponential of the particular distribution component as shown in **Fig. 4B**.

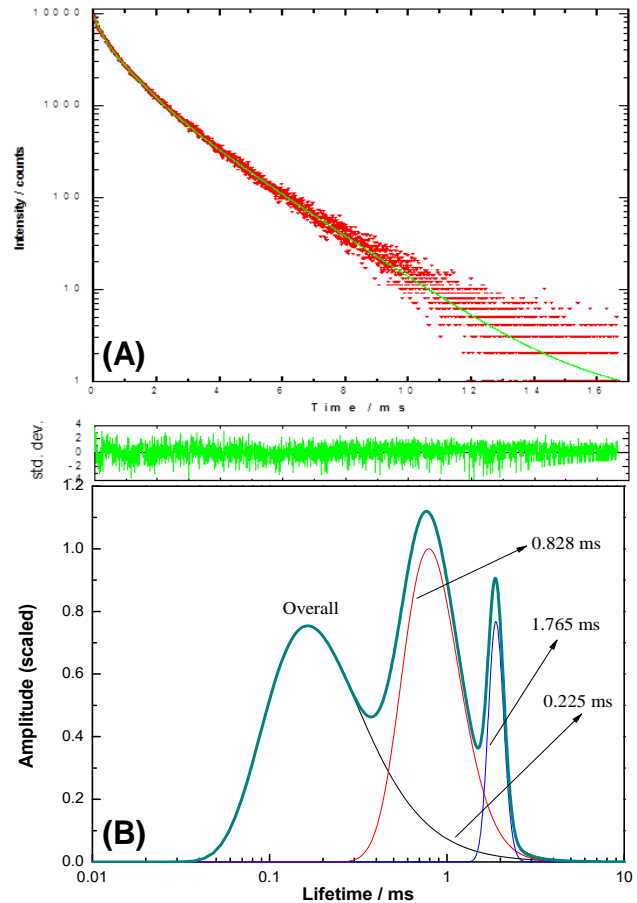


Fig. 4 (A) Decay curves (life times) (i.e. sum decays) of simple exponential; (B) Lifetimes data by NED distribution analysis of 2Sm calcium phosphate host glass.

Time-resolved emission profiles of Sm^{3+} doped calcium phosphate host glass

Time-resolved luminescence spectroscopy can be very useful in samples that present many emitting centres simultaneously. With the steady state (intensity only) techniques there may be an observational bias towards the more intense or longer-lived centres, while others remain unnoticed [30]. It is possible to quantify time resolved emission by the following equation:

$$Em_{ba}(\omega, t) = \sum_{v'} Em_{bv'}(\omega) X_{bv'}(t) \quad (5)$$

where, $Em_{bv'}$ denotes the emission intensity distribution function of the vibronic state b , being v' its associated

vibrational quantum number. X_{bv} is the concentration of molecules in the state b [31]. The functions in the Eq. (5) are not easily determined. However, it is possible to verify that for a given t and an electronic state, if X_{bv} is small or inexistent, the contribution for overall emission is null. Therefore, it is possible to study the different luminescent centres in a sample based on their lifetimes. In Fig. 5 shows the decay associated spectra for the 2Sm glass emission spectra obtained from a global analysis of the TRES data, modelled as the sum of exponentials. Since each of the decay associated spectra exhibit the same wavelength response this can imply that they share the same transition origin, however the local host environment can exert an influence on the observed decays times.

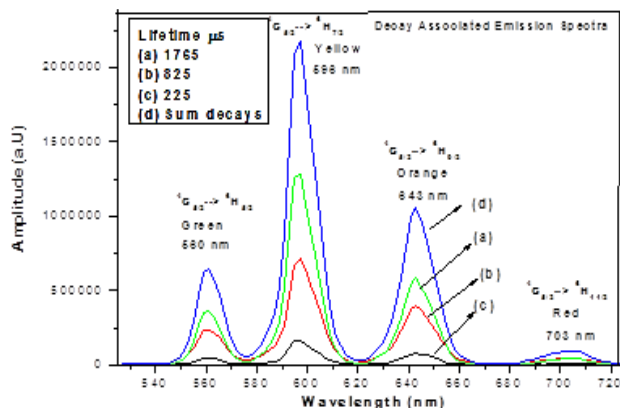


Fig. 5. Decay associated spectra (DAS) showing the emission spectra obtained for different lifetimes of (a) 1765 μ s, (b) 825 μ s, (c) 225 μ s and (d) sum decays for 2Sm calcium phosphate host glass.

Conclusion

In summary, it is concluded that the spectral results clearly demonstrate the dependence of the emission spectra of the 2Sm glass on the excitation wavelength. It is found that 259nm and 405nm excitation wavelengths could be suggested as the ideal pump wavelengths in achieving stronger luminescence performance from this optical glass. Hence this glass could be considered as luminescent optical glass exhibiting the yellow-orange colour ${}^4G_{5/2} \rightarrow {}^6H_{7/2} & {}^6H_{9/2}$ for potential application in the development of luminescent glass systems. Furthermore, two NIR peaks at 1134 nm (${}^4G_{5/2} \rightarrow {}^6F_{11/2}$) and 1310 nm (${}^4G_{5/2} \rightarrow {}^6F_{9/2}$) are monitored by using an excitation source at 1060nm. According to the best of our knowledge, this is first time, we reported two NIR peaks for the 2 Sm calcium phosphate host glass. By using the time-resolved emission (TRES) it is possible to obtain more quantifiable data. Analysis of these data enable the decay associated spectra to be obtained. This gives both the information concerning the energy of the transition as well as its decay kinetic. Additional studies are underway to study up-conversion phenomena of 2Sm doped calcium phosphate glass for their technological importance in the development of laser glass material in bio-imaging applications.

Acknowledgements

The authors would like to acknowledge the financial support from the European Union's Seventh Framework Programme (FP7/2007-2013) under grant agreement n^o REGPOT-CT2012-316331-POLARIS. Also,

SHN would like to thank to Cost Action, ref. # MP 1205 under materials (soft, bio & nano) and technologies for optofluidic devices, and further acknowledge to the FCT -*Fundação para a Ciência e a Tecnologia*, Portugal, through the project PTDC/SAU-BEB/103034/2008.

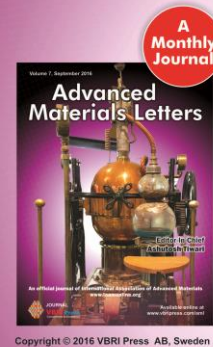
Author contributions

All authors contributed equally to the work. Authors have no competing financial interests.

References

- Sooraj Hussain, N.; *et al.*; Calcium phosphate-based materials for Bone Regenerative Medicine, In *Biomaterials for Bone Regenerative Medicine*; Sooraj Hussain, N; Santos, J.D. (Eds.); *Trans Tech Publisher*: Switzerland, **2010**, pp. 153.
- Barta, C. A.; Sachs-Barrable, K.; Jia, J.; Thompson, K. H.; Wasan, K. M.; Orvig, C.; *Dalton Trans.*, **2007**, *43*, 5019. DOI: [10.1039/b705123a](https://doi.org/10.1039/b705123a)
- Durbin, P. W.; Williams, M. H.; Gee, M.; Newman, R. H.; Hamilton, J. G; *Proc. Soc. Exp. Biol. Med.*, **1956**, *91*, 78. DOI: [10.3181/00379727-91-22175](https://doi.org/10.3181/00379727-91-22175)
- Sooraj Hussain, N.; Santos, J.D. (Eds.); *Trans Tech Publisher*, Switzerland, **2008**.
- Gschneidner, Jr K.A.; Eyring, L. (Eds); Elsevier, USA, **1998**.
- Fricker, S. P.; *Chem. Soc. Rev.*, **2006**, *35*, 524. DOI: [10.1039/b509608c](https://doi.org/10.1039/b509608c)
- J. Zhang, J., Y. Li, Y., et.al; *Mini. Rev. Med. Chem.*, **2011**, *11*, 678. DOI: [10.2174/1389557111796268804](https://doi.org/10.2174/1389557111796268804)
- www.platcomventures.com/techprofile_a_method_for_the_production_of_lanthanide_substituted_calcium_phosphate_biomaterial.aspx, Project code: P 300.
- Coelho, J.; *et al.*; Development and characterization of lanthanides-doped hydroxyapatite composites for bone tissue application, In *Current Trends on Glass and Ceramics Materials*, Sooraj Hussain, N; Santos, J.D. (Eds.); *Bentham Science Publishers*, UAE, **2013**, pp 87.
- Morais, D.S.; Fernandes, S.; *et al.*, *Biomed. Mater.*, **2015**, *10*, 055008. DOI: [10.1088/1748-6041/10/5/055008](https://doi.org/10.1088/1748-6041/10/5/055008)
- Morais, D.S.; Coelho, J.; et.al; *J. Mater. Chem. B*, **2014**, *2*, 5872. DOI: [10.1039/C4TB00484A](https://doi.org/10.1039/C4TB00484A)
- Chenzhong, Y.; Yexiang, T.; *TRAC- Trend Anal. Chem.*, **2012**, *39*, 60. DOI: [10.1016/j.trac.2012.07.007](https://doi.org/10.1016/j.trac.2012.07.007)
- Sooraj Hussain, N. *et al.* Luminescence Spectra of rare-earth ions doped Zinc-Boro Silicate and Lead- Bismuth-Germanate Glasses, In *Physics and Chemistry of Rare earth ions doped glasses*. Sooraj Hussain, N; Santos, J.D. (Eds.); *Trans Tech Publisher*: Switzerland **2008**, 225.
- Kindrat, I.I.; Padyak, B.V.; Drzewiecki, A.; *J. Lumin.*, **2015**, *166*, 264. DOI: [10.1016/j.jlumin.2015.05.051](https://doi.org/10.1016/j.jlumin.2015.05.051)
- Ramteke, D.D.; Annapurna, K.; Deshpande, V.K.; Gedam, R.S. *J. of Rare Earths*, **2014**, *32*, 1148. DOI: [10.1016/S1002-0721\(14\)60196-4](https://doi.org/10.1016/S1002-0721(14)60196-4)
- Ramteke, D. D.; Ganvir, V.Y.; Munishwar, S. R.; Gedam, R. S., *Physics Procedia*, **2015**, *76*, 25. DOI: [10.1016/j.phpro.2015.10.005](https://doi.org/10.1016/j.phpro.2015.10.005)
- Sooraj Hussain, N.; Prabhakar Reddy, Y.; Buddhudu, S; *J. Mat. Sci.Lett.* **2002**, *21*, 397. DOI: [10.1023/A:1014963402945](https://doi.org/10.1023/A:1014963402945)
- Sooraj Hussain, N.; Hungerford, G.; et.al; *J. Nanosci. Nanotech.* **2009**, *9*, 3672. DOI: [10.1166/jnn.2009.NS49](https://doi.org/10.1166/jnn.2009.NS49)
- Damas, P.; Coelho, J.; Hungerford, G.; Sooraj Hussain, N; *Mater. Res. Bulletin*, **2012**, *47*, 3489. DOI: [10.1016/j.materresbull.2012.06.071](https://doi.org/10.1016/j.materresbull.2012.06.071)
- Coelho, J.; Hungerford, G.; Sooraj Hussain, N; *Chem. Phys. Lett.* **2011**, *512*, 70. DOI: [10.1016/j.cplett.2011.07.019](https://doi.org/10.1016/j.cplett.2011.07.019)
- Coelho, J.; Hungerford, G.; Sooraj Hussain, N; *Solid State Phenomena*, **2014**, *207*, 37.
- Venkateswara Rao, G., Shashikala, H.D; *Glass Phys. Chem.*, **2014**, *40*, 303. DOI: [10.1134/S1087659614030249](https://doi.org/10.1134/S1087659614030249)

23. Roiland C, Fayon F, Simon P, Massiot D; *J Non-Cryst Solids*, **2011**, 357,1636.
DOI: [10.1016/j.jnoncrysol.2011.01.023](https://doi.org/10.1016/j.jnoncrysol.2011.01.023)
24. Hudgens, J.J.; Brow, R.K.; Tallant, D.R.; Martin, S.W; *J. Non-Cryst Solids*, **1998**, 223, 21.
DOI: [10.1016/S0022-3093\(97\)00347-5](https://doi.org/10.1016/S0022-3093(97)00347-5)
25. Vedeau, N.; Cozar, O.; et al.; *Vib Spectrosc.*, **2008**, 48, 259.
DOI: [10.1016/j.vibspec.2008.01.003](https://doi.org/10.1016/j.vibspec.2008.01.003)
26. Marzouk, M.A.; Hamdy, Y.M.; et al; *J.Lumin.*, **2015**, 166, 295.
DOI: [10.1016/j.jlumin.2015.05.054](https://doi.org/10.1016/j.jlumin.2015.05.054)
27. Tsallis, C; *Braz. J. Phys.*, **2009**, 39, 337.
DOI: [10.1590/S0103-97332009000400002](https://doi.org/10.1590/S0103-97332009000400002)
28. J. Włodarczyk, J.; Kierdaszuk, B.; *Biophys. J.*, **2003**, 85, 589.
DOI: [10.1016/S0006-3495\(03\)74503-2](https://doi.org/10.1016/S0006-3495(03)74503-2)
29. Rolinski, O.J.; D.J.S. Birch; *J. Chem. Phys.*, **2008**, 129, 144507.
DOI: [10.1063/1.2990651](https://doi.org/10.1063/1.2990651)
30. Gaft M.; Reisfeld, R.; Panczer, G. (Eds.); *Luminescence spectroscopy of minerals and materials*; Springer Verlag; Switzerland, **2005**.
DOI: [10.1007/978-3-319-24765-6](https://doi.org/10.1007/978-3-319-24765-6)
31. Fleming, G.R.; Gijzeman O. L. J.; et al.; *J Chem Soc, Faraday Trans.*, **1975**, 2, 773.
DOI: [10.1039/F29757100773](https://doi.org/10.1039/F29757100773)



A Monthly Journal

Advanced Materials Letters

Volume 7, September 2016

Publish your article in this journal

Advanced Materials Letters is an official international journal of International Association of Advanced Materials (IAAM, www.iaamonline.org) published monthly by VBRI Press AB from Sweden. The journal is intended to provide high-quality peer-review articles in the fascinating field of materials science and technology particularly in the area of structure, synthesis and processing, characterisation, advanced-state properties and applications of materials. All published articles are indexed in various databases and are available download for free. The manuscript management system is completely electronic and has fast and fair peer-review process. The journal includes review article, research article, notes, letter to editor and short communications.

Copyright © 2016 VBRI Press AB, Sweden

www.vbripress.com/aml